Structural Engineering and Mechanics, Vol. 28, No. 2 (2008) 153-166
DOI: http://dx.doi.org/10.12989/sem.2008.28.2.153

Application of wavelet multiresolution analysis and artificial intelligence for generation of artificial earthquake accelerograms

G. Ghodrati Amiri† and A. Bagheri‡

Center of Excellence for Fundamental Studies in Structural Engineering, College of Civil Engineering, Iran University of Science & Technology, PO Box 16765-163, Narmak, Tehran 16846, Iran

(Received August 16, 2006, Accepted October 2, 2007)

Abstract. This paper suggests the use of wavelet multiresolution analysis (WMRA) and neural network for generation of artificial earthquake accelerograms from target spectrum. This procedure uses the learning capabilities of radial basis function (RBF) neural network to expand the knowledge of the inverse mapping from response spectrum to earthquake accelerogram. In the first step, WMRA is used to decompose earthquake accelerograms to several levels that each level covers a special range of frequencies, and then for every level a RBF neural network is trained to learn to relate the response spectrum to wavelet coefficients. Finally the generated accelerogram using inverse discrete wavelet transform is obtained. An example is presented to demonstrate the effectiveness of the method.

Keywords: artificial accelerogram; wavelet transform; RBF neural network; target spectrum.

1. Introduction

For seismic design of structures, a dynamic analysis, either response spectrum or time- history analysis is often required. The major imperfect of response spectrum analysis in seismic design of structures lies in its debility to provide temporal information of the structural responses. Such information is sometimes necessary in achieving a satisfactory design. In many cases, house equipment is sensitive to floor vibrations during an earthquake. It is sometimes necessary to develop response of the floor. In addition, when designing critical or major structures such as power plants, dams, and high-rise buildings, the final design is usually based on the complete time-history analysis. To provide input excitations to structural models for sites with no strong ground motion data, it is necessary to generate artificial accelerograms (Fan and Ahmadi 1990).

The best accelerogram is one, which has compatible characteristics with desired area. Therefore, it is difficult or may be impossible in some cases to choose a proper record for a design area, because the recorded and processed accelerograms of the design location are few. Besides, other location records do not satisfy the geo-seismic characteristics on desired location. In this case, artificial earthquakes that are statistically generated based on desired properties are very useful for analysis or

† Professor, Corresponding author, E-mail: ghodrati@iust.ac.ir.
‡ Graduate Student, E-mail: abaghery@civil.eng.iust.ac.ir

design operation.

The newly developed wavelet analysis has emerged as a powerful tool to analyze temporal variations in frequency content. Recent applications of the wavelet transform to engineering problems can be found in several studies that refer to dynamic analysis of structures, damage detection, system identification, etc. Newland (1994) applied wavelets for analyzing vibration signals, and developed special wavelets and techniques for engineering purpose. Iyama and Kuwamura (1999), Mukherjee and Gapta (2002), Zhou and Adeli (2003), Rajasekaran *et al*. (2006), and Ghodrati Amiri *et al.* (2006) developed the wavelet analysis for generating earthquake accelerograms.

A design spectrum is used in structural design very often. The artificially generated earthquake accelerograms must be compatible with the design spectrum, i.e. their response spectrum of the generated accelerogram must closely approximate the design spectrum. Recently, Ghaboussi and Lin (1998), Lin and Ghaboussi (2000) and Lee and Han (2002) have developed innovative methodologies for generating artificial earthquake accelerograms using neural network.

Ghodrati Amiri *et al.* (2006) purposed to generate many artificial records compatible with the same spectrum by wavelet theory. But in this paper the decomposing capabilities of wavelet transform and the learning abilities of RBF neural network are used to develop a method for generating accelerograms from response spectra. The proposed method is validated by using 106 accelerograms to train the RBF neural networks. The performance of the trained RBF neural network is estimated by generating accelerogram for new response spectra.

2. Wavelet theory

2.1 Basis function

Fast Fourier transform (FFT) is an excellent tool for finding the frequency components of a signal. A disadvantage of the FFT is that frequency components can only be extracted from the complete duration of a signal. The frequency components are obtained from an average over the whole length of the signal. Therefore it is not a suitable tool for a non-stationary signal such as the impulse response of cracked beams, vibration generated by faults in a gearbox, and structural response to wind storms, just to name a few. These types of problems associated with FFT can be resolved by using wavelet analysis. It provides a powerful tool to characterize local features of a signal. Unlike Fourier transform, where the function used as the basis of decomposition is always a sinusoidal wave, other basis functions can be selected for wavelet shape according to the features of the signal. The basis function in wavelet analysis is defined by two parameters named scale and translation. This property leads to a multi-resolution representation for non-stationary signals. As mentioned before, a basis function (or mother wavelet) is used in wavelet analysis. For a wavelet of order N, the basis function can be represented as

$$\psi(n) = \sum_{j=0}^{N-1} (-1)^j c_j (2n + j - N + 1) \tag{1}$$

Where c_j is jth coefficient. The basis function should satisfy the following two conditions (Relations (2) and (3)):

The basis function integrates to zero, i.e.

$$\int_{-\infty}^{+\infty} \psi(t)\,dt = 0 \tag{2}$$

It is square integrable or, equivalently, has finite energy, i.e.

$$\int_{-\infty}^{+\infty} |\psi(t)|^2\,dt < \infty \tag{3}$$

Eq. (2) suggests that the basis function be oscillatory or have a wavy shape. Eq. (3) implies that most of the energy in the basis function is confined to a finite duration. The important properties of basis functions are 'orthogonality' and 'biorthogonality'. These properties make it possible to calculate the coefficients very efficiently. There is no redundancy in the sense that there is only one possible wavelet decomposition for the signal being analyzed. However, not all basis functions have these properties. A frequently mentioned term in the definition of a basis function is 'compact support', which means that the values of the basis function are non-zero for finite intervals. This property enables one to efficiently represent signals that have localized features.

2.3. Discrete wavelet transform (DWT)

The main idea of DWT is the same as that of continuous wavelet transform (CWT). While CWT requires much calculation effort to find the coefficients at every single value of the scale parameter, DWT adopts dyadic scales and translations (i.e., scales and translations based on powers of two) in order to reduce the amount of computation, which results in better efficiency of calculation. Filters of different cutoff frequencies are used for the analysis of the signal at different scales. The signal is passed through a series of high-pass filters to analyze high frequencies, and through a series of low-pass filters to analyze low frequencies. In DWT the signals can be represented by approximations and details. The detail at level j is defined as

$$D_j(t) = \sum_{k \in Z} cD_{j,k}\,\psi_{j,k}(t) \tag{4}$$

Where Z is the set of positive integers and $cD_{j,k}$ is *wavelet Coefficients* at level j which is defined as

$$cD_j(k) = \int_{-\infty}^{\infty} f(t)\psi_{j,k}(t)\,dt \tag{5}$$

The approximation at level j is defined as

$$A_j(t) = \sum_{k=-\infty}^{\infty} cA_j(k)\,\phi_{j,k}(t) \tag{6}$$

Where $cA_{j,k}$ is *scaling Coefficient*s at level j which is defined as

$$cA_j(k) = \int_{-\infty}^{\infty} f(t)\phi_{j,k}(t)\,dt \tag{7}$$

Finally, the signal $f(t)$ can be represented by

$$f(t) = A_J + \sum_{j \le J} D_j \tag{8}$$

As opposed to CWT where only a wavelet function is used, in DWT a scaling function is used, in addition to the wavelet function. These are related to low-pass and high-pass filters, respectively. The scaling function can also be represented as

$$\phi(n) = \sum_{j=0}^{N-1} c_j \phi(2n - j) \tag{9}$$

$$\phi_{j,k}(n) = 2^{j/2} \phi(2^j t - k) \tag{10}$$

Not all wavelet functions have scaling functions. Only orthogonal wavelets have their scaling functions. This DWT can be very useful for on-line health monitoring of structures, since it can efficiently detect the time of a frequency change caused by stiffness degradation. Further details about wavelet theory can be found in Daubechies (1992).

Since, each $D_j(t)$ has a range of particular out of which the intensity is zero, a supposition is introduced here that the original function $f(t)$ is decomposed into a series of $D_j(t)$'s exclusively in frequency domain. In other word, each $D_j(t)$ has non-zero components only in an exclusive range of frequency. This supposition is not theoretically exact but is justified later from a viewpoint of engineering practice. The exclusive range of frequency of $D_j(t)$ is denoted as follows

$$\text{frequency range of level } j = [f_{1j}, f_{2j}] \tag{11}$$

or

$$\text{period range of level } j = [T_{1j}, T_{2j}] \tag{12}$$

From the nature of discrete wavelet transform that $D_j(t)$ has components of half frequency of $D_{j+1}(t)$ (Benedetto and Frazier 1994), f_{1j}, f_{2j}, T_{1j} and T_{2j} are expressed as follows

$$f_{1j} = 2^{-j-1}/\Delta t, \qquad f_{2j} = 2^{-j}/\Delta t \tag{13}$$

$$T_{1j} = 2^{j}/\Delta t, \qquad T_{2j} = 2^{j+1}/\Delta t \tag{14}$$

where t is the time step of digital data of $f(t)$.

3. RBF neural networks

RBF neural networks are feed-forward networks trained using a supervised training algorithm. They are typically configured with a single hidden layer of units whose activation function is selected from a class of functions called basis functions. While similar to back propagation in many respects, radial basis function networks have several advantages. They usually train much faster than back propagation networks. They are less susceptible to problems with non-stationary inputs because of the behavior of the radial basis function hidden units.

RBF neural networks have proven to be useful neural network architecture. The major difference between RBF networks and back propagation networks (that is, multi layer perceptron trained by Back Propagation algorithm) is the behavior of the single hidden layer. Rather than using the

sigmoidal or S-shaped activation function as in back propagation, the hidden units in RBF networks use a Gaussian or some other basis Kernel function (Park and Sandberg 1991). Each hidden unit acts as a locally tuned processor that computes a score for the match between the input vector and its connection weights or centers. In effect, the basis units are highly specialized pattern detectors. The weights connecting the basis units to the outputs are used to take linear combinations of the hidden units to produce the final classification or output.

4. Proposed method

The studies of Fourier, energy, power, and response spectra show that though the pattern of different earthquake records are not similar even in an specified area, but a certain pattern of response spectra could often be attained for the specified area because of their similarities (Ghaboussi and Lin 1998, Lin and Ghaboussi 2000). In fact, a design spectrum is derived by smoothing according to geophysical and geotechnical parameters. The problem is that design spectrum may derive from different records which are related to different accelerograms of that location. Therefore, it is easy to calculate the spectra, but the inversion operation to attain an artificial record is almost impossible. So it should be calculated with a non-classic method and then compared with target spectrum at the end. In this case, the artificial record has to satisfy static analysis conditions, therefore the related spectrum should be approximately equal to design spectrum.

It is ideal to develop an artificial earthquake accelerogram, compatible with a given response spectrum. The need for expanding accelerograms from response spectra is increasing. If we consider determining the spectra from accelerograms as a direct problem, then, determining the accelerograms from their spectra is an inverse problem. In the case of the Fourier spectra, the mapping is reversible and the inverse problem can be uniquely solved. However, in the case of response spectrum, the mapping is not uniquely reversible. In calculating the response spectrum from an accelerogram meaningful amount of information in the accelerogram gets lost, thus, to generate it mathematically is impossible to uniquely recover the accelerogram. Nevertheless, it may be possible to expand one or several accelerograms whose response spectra are about to a given response spectrum.

The main objective of this paper is to present a new method based on wavelet theory and RBF neural network to generate artificial accelerogram which has a response spectrum close to a specified response spectrum used as input of neural network. Moreover, the accelerogram generated from a given response spectrum should either have characteristics like to the group of accelerograms used in the training of the neural network.

The proposed method is based on expanding a RBF neural network which takes the discretized ordinates of the pseudo-velocity response spectra of period range at level j of the DWT as input, and the output of the RBF neural networks produces the wavelet coefficients at level j of the DWT of the earthquake accelerograms. The input layer of RBF network j has the pseudo-velocity response spectrum at period range of level j of the DWT

$$PSV_j(\omega, \xi) = \frac{2\pi}{T} \max_t |x(t)|, \qquad T_{1j} \le T \le T_{2j} \tag{15}$$

$$\ddot{x}(t) + 2\xi\omega\dot{x}(t) + \omega^2 x(t) = -a_g(t) \tag{16}$$

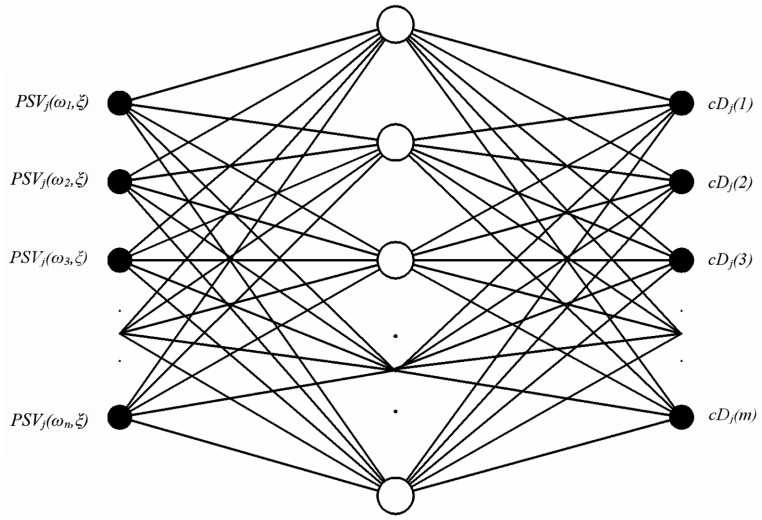

Fig. 1 The architecture of RBF neural network *j*

Where ω, ξ and $a_g(t)$ are the fundamental frequency and the damping coefficient of the single degree of freedom system (SDOF) and the earthquake ground acceleration, respectively. In this study the earthquake ground acceleration is decomposed with DWT to level 7; therefore, there will be eight RBF neural networks. If records have Δt = 0.02 sec, the input layers have 5, 9, 17, 33, 65, 129, 257 and 513 nodes for RBF networks 1 to 8.

The output layer of RBF network *j* has *cD* at level *j* of the DWT of the earthquake accelerograms. If records have 2^{11} = 2048 points, the output layers have 1033, 526, 272, 145, 82, 50 and 34 nodes for RBF networks 1 to 8. Fig. 1 shows the architecture of RBF neural network *j*.

Finally after training of the RBF networks, the generated accelerograms using inverse discrete wavelet transform is obtained. 106 earthquake accelerograms used in the training of the RBF networks.

5. An illustrative example

This study has been accomplished for 106 selected records of Iran (Ramezi 1997). Table 1 shows list of training and testing records for neural network. These records were scaled with their peak ground acceleration to 1g. In this section, the proposed method has been applied with MATLAB software (MATLAB 1999) for neural networks. In this study all records have Δt = 0.02 sec, and 2^{11} = 2048 points consequently. Therefore a series of zeros is added to the records which are shorter than desired length (2048 × 0.02 = 40.96 sec) to gain proper length and for the longer ones, the strong duration of records of longer length is considered according to MacCann and Shah algorithm (MacCann and Shah 1979).

All pseudo-velocity response spectra are calculated with 5 percent damping (Naeim 1999). It is noted that the records have been decomposed with db-10 wavelet. Also the other wavelets could have been applied.

The eight RBF neural networks were trained with response spectra and the wavelet coefficients of

Table 1 List of training and testing records for neural network

Number	Occurance date	Name of station	Magnitude (m_b)	Modified PGA (cm/s^2)	Duration (Sec)
1	1975.03.07	Bandar Abbas-2	5.9	83	45.34
2	1975.03.07	Minam	5.9	28	28.44
3	1976.11.07	Ghaen	5.8	170	19.54
4	1976.11.07	Khezri	5.8	25	21.02
5	1976.11.24	Maku	6.2	86	28.06
6	1976.11.09	Klat-e-alam	5.1	34	19.88
7	1977.03.21	Bandar Abbas-2	6.2	90	45.22
8	1977.03.21	Bandar Abbas-2	5.7	34	21.30
9	1977.03.23	Bandar Abbas-2	5.7	33	17.48
10	1977.04.01	Bandar Abbas-1	5.9	41	30.80
11	1977.04.06	Naghan-1	5.4	700	20.96
12	1978.09.16	Deyhook	6.5	272	58.38
13	1978.09.16	Tabas	6.7	832	49.00
14	1978.09.16	Tabas	4.9	119	12.38
15	1978.09.17	Tabas	4.6	124	19.02
16	1978.09.19	Tabas	4.7	143	15.26
17	1978.09.16	Tabas	4.7	141	15.24
18	1979.01.16	Bajestan	6.0	40	15.60
19	1979.01.16	Khaf	6.0	69	32.42
20	1980.07.22	Lahijan	5.3	55	13.66
21	1981.07.28	Rayen	5.9	30	43.02
22	1981.07.28	Golbaf	5.9	244	59.32
23	1981.07.28	Zarand	5.9	41	43.88
24	1981.07.28	Ravar	5.9	63	14.44
25	1981.08.08	Golbaft	4.8	99	13.84
26	1981.10.14	Golbaft	5.2	97	17.00
27	1980.12.03	Golbaft	5.1	102	18.98
28	1984.06.01	Ardal	5.0	137	15.60
29	1987.04.10	Esferayen	5.0	124	18.12
30	1988.08.11	Kazerun	5.6	42	17.96
31	1988.12.06	Nurabadmamasani	5.5	85	17.28
32	1989.03.15	Ardal	4.6	143	19.96
33	1989.11.20	Sirch	5.5	63	18.60
34	1990.06.20	Abhar	6.4	127	29.48
35	1990.06.20	Rudsar	6.4	91	53.10
36	1990.06.20	Lahijan	6.4	111	60.54
37	1990.06.20	Tonekabon	6.8	130	35.94
38	1990.06.24	Manjil	5.1	416	11.00
39	1990.06.20	Abbar	6.4	410	58.16
40	1990.06.20	Zanjan	6.4	125	59.78
41	1990.07.06	Manjil	5.2	163	9.54
42	1990.08.21	Manjil	4.8	106	9.84
43	1990.08.20	Rudbar-1	4.8	292	14.12
44	1990.08.21	Rudbar-1	4.8	184	13.36

Table 1 Continued

Number	Occurance date	Name of station	Magnitude (m_b)	Modified PGA (cm/s^2)	Duration (Sec)
45	1990.08.27	Rudbar-1	4.7	50	11.44
46	1990.09.25	Manjil	4.9	49	14.50
47	1991.11.28	Rudbar-1	5.7	268	19.94
48	1991.12.04	Rudbar-1	4.3	126	12.54
49	1994.03.30	Firuzabad	5.5	60	12.98
50	1994.03.30	Zarrat	5.5	196	33.24
51	1994.06.18	Zarrat	5.1	96	25.56
52	1994.06.20	Zarrat	5.9	289	43.50
53	1994.06.20	Firuzabad-1	5.9	235	38.36
54	1994.03.17	Zanjiran	4.8	61	15.34
55	1994.06.05	Zanjiran	4.5	172	21.72
56	1994.06.18	Zanjiran	5.1	84	24.28
57	1994.06.20	Zanjiran	5.9	841	63.98
58	1994.12.08	Zarrat	5.0	58	20.44
59	1995.04.26	Rudbar	4.8	89	17.88
60	1995.04.26	Sefidrud Dam(U)	6.4	125	59.78

the earthquake accelerograms in the training set. The trained neural network was tested with the earthquake accelerograms from the training set. Figs. 2-4 show the performance of the trained neural network on three of the earthquake accelerograms from the training set. For example, Fig. 2 shows the time history of Naghan 1977 earthquake at the top of the figure. The middle part of Fig. 2 shows the generated accelerogram and the bottom part of Fig. 2 shows the pseudo-acceleration response spectra of original and generated accelerogram. Comparison of the input and output accelerograms and their pseudo-acceleration response spectra clearly display that the trained neural networks has learnt the training cases very good. Figs. 3 and 4 show similarly comparisons for Tabas 1978 and Khaf 1979 earthquakes. The three earthquakes in Figs. 2-4, evidently have different characteristics and trained neural network performs equally well in generating these earthquakes from their response spectra.

In case there are no earthquake accelerograms in the neural network's training set which have a response spectrum close to the input response spectrum, the trained neural network generates a reasonable accelerogram shape from its training set. Figs. 5-7 show three such cases. In Fig. 5 the input to the neural network is the response spectrum of Zarrat 1994 earthquake, and the generated accelerogram is shown in the middle part of the figure. The generated accelerogram is very close to the Zarrat earthquake record. Figs. 6 and 7 show simillarly comparisons for Rodsar 1991 and Zanjeeran 1994 earthquakes. From these three examples it is reasonable to conclude that the trained neural network is able of generating accelerograms for any novel response spectra.

Finally, it is interesting to determine whether the trained neural network is able of generating reasonable accelerograms from design spectra. In Fig. 8, the training neural network is furnished with a design response spectrum as input, and the generated accelerogram is shown in the top portion of the figure. This is a useful property of the neural network based method, in that it will enable generation of accelerograms compatible with any defined design spectra.

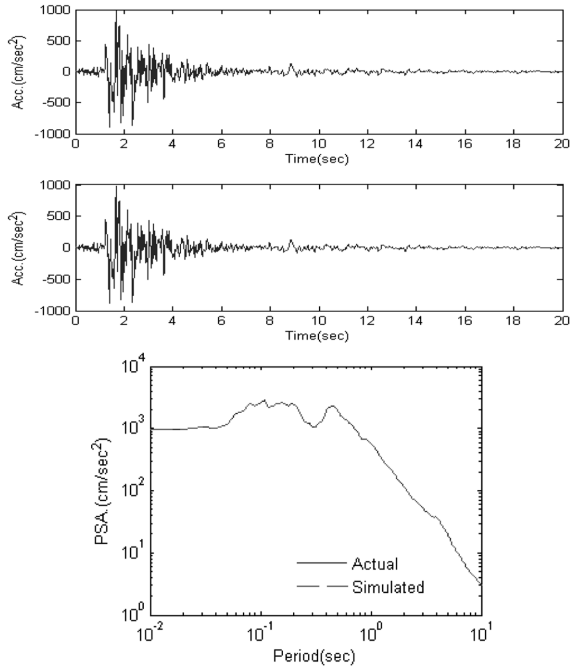

Fig. 2 Accelerogram of Naghan 1977 earthquake (top), neural network generated accelerogram (middle) and comparison between pseudo-acceleration response spectra of original and generated accelerograms (below)

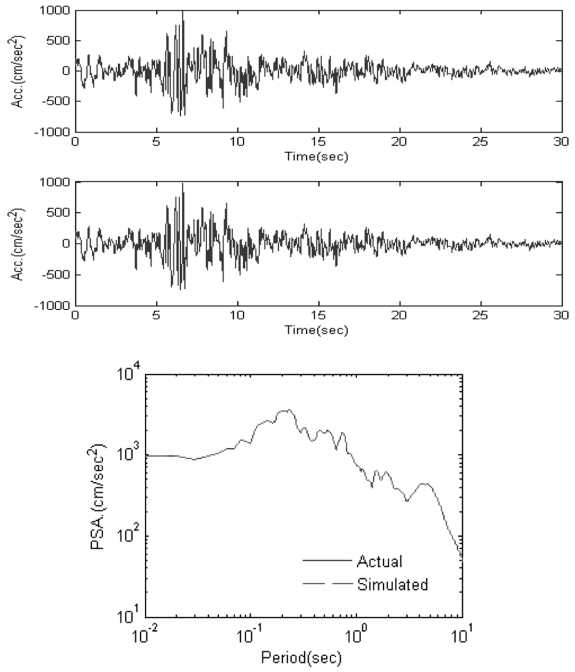

Fig. 3 Accelerogram of Tabas 1978 earthquake (top), neural network generated accelerogram (middle) and comparison between pseudo-acceleration response spectra of original and generated accelerograms (below)

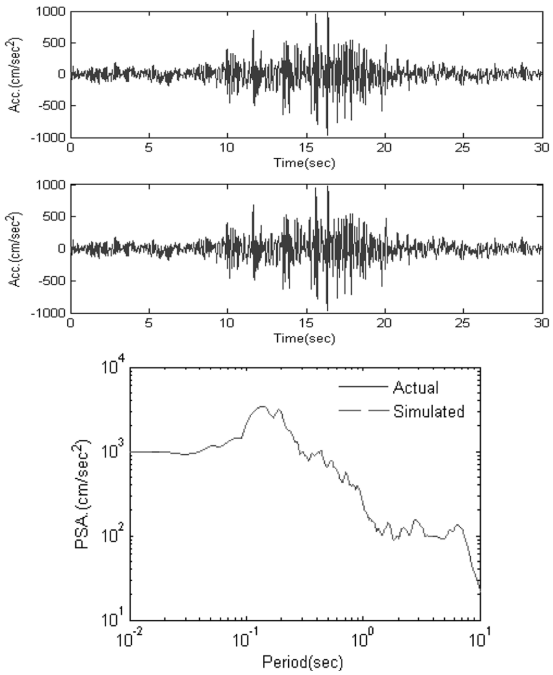

Fig. 4 Accelerogram of Khaf 1979 earthquake (top), neural network generated accelerogram (middle) and comparison between pseudo-acceleration response spectra of original and generated accelerograms (below)

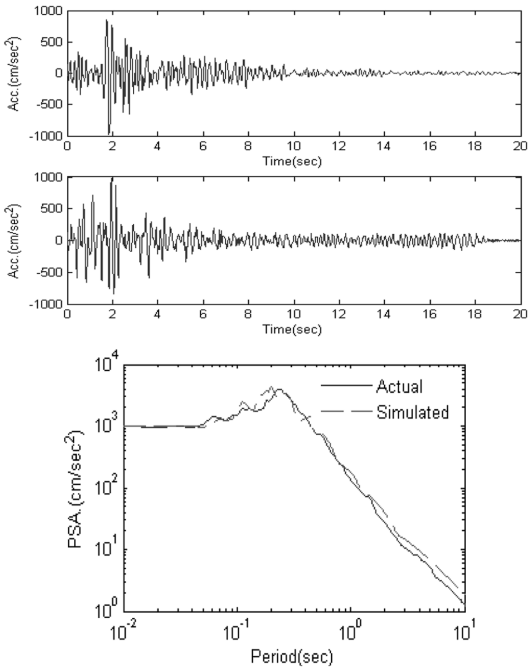

Fig. 5 Accelerogram of Zarrat 1994 earthquake (top), neural network generated accelerogram (middle) and comparison between pseudo-acceleration response spectra of original and generated accelerograms (below)

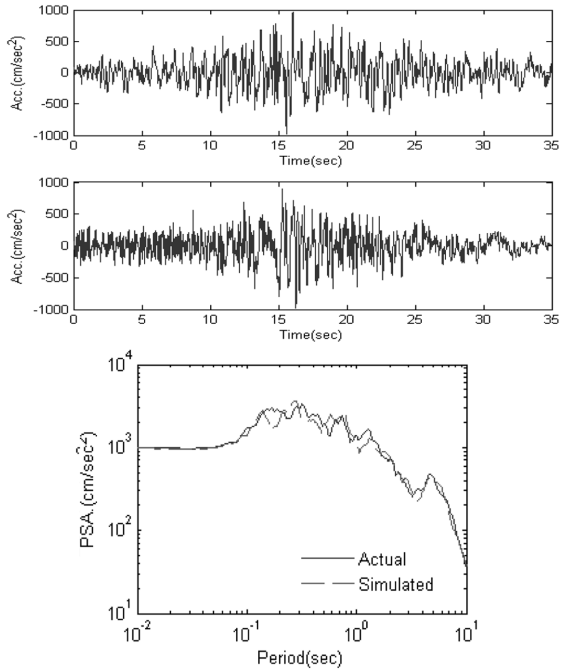

Fig. 6 Accelerogram of Roudsar 1991 earthquake (top), neural network generated accelerogram (middle) and comparison between pseudo-acceleration response spectra of original and generated accelerograms (below)

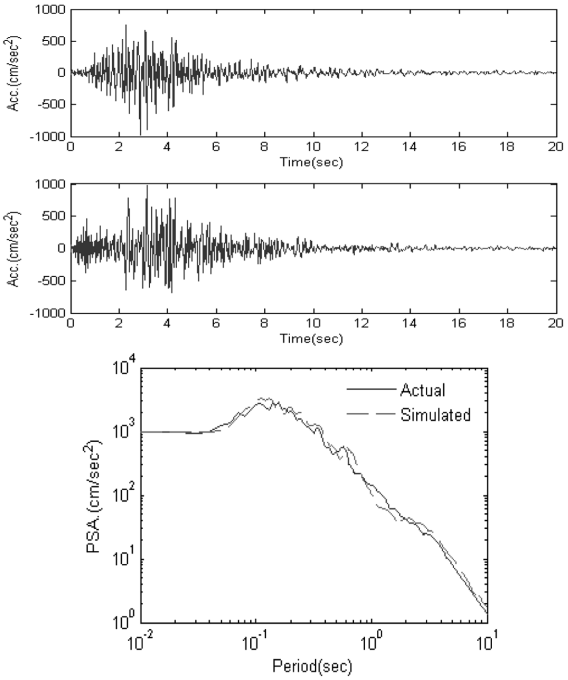

Fig. 7 Accelerogram of Zanjeeran 1994 earthquake (top), neural network generated accelerogram (middle) and comparison between pseudo-acceleration response spectra of original and generated accelerograms (below)

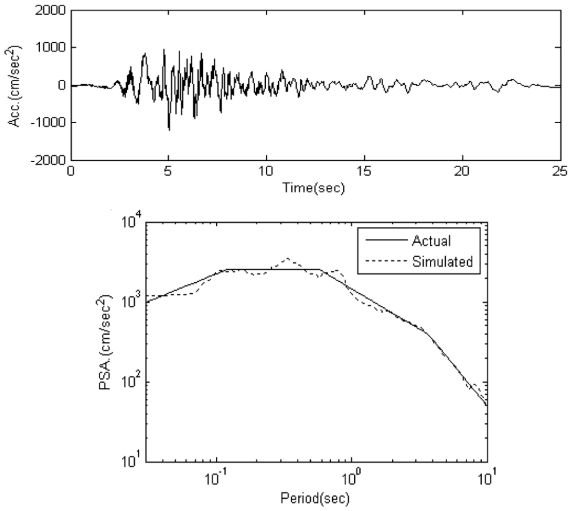

Fig. 8 Neural network generated accelerogram (top) and comparison between design spectrum with pseudo-acceleration response spectrum (below)

6. Conclusions

In this study, a method of applying wavelet transform and neural network for generation of artificial accelerograms from pseudo-velocity response spectra is developed. First DWT is used to decompose earthquake accelerograms to several levels that each level covers a special range of frequencies, and then for every level a RBF neural network is trained to learn to relate the response spectrum to wavelet coefficients. Finally the generated accelerogram using inverse discrete wavelet transform is obtained. In an illustrative example, the proposed method was applied to a sample of 106 recorded earthquake accelerograms. In testing the trained neural networks, it was fund out that, when given a pseudo-velocity response spectrum as input, the generated neural network either generates an accelerograms very similar to one from its training set; one which has a pseudo-velocity response spectrum close to input, or it synthesizes a new and realistic looking accelerogram. The proposed method was also tested by using design spectra as input and generating accelerograms compatible with those spectra.

References

Benedetto, J.J. and Frazier, M.W. (1994), *WAVELETS: Mathematics and Applications*, CRC Press, Boca Raton.

Daubechies, I. (1992), "Ten lectures on wavelets", *CBMS-NSF Conference Series in Applied Mathematics*, Montpelier, Vermont.

Fan, F.G. and Ahmadi, G. (1990), "Nonstationary Kanai-Tajimi models for El Centro 1940 and Mexico City 1985 earthquake", *Probab. Eng. Mech.*, **5**, 171-181.

Ghaboussi, J. and Lin., C.J. (1998), "New method of generating spectrum compatible accelerograms using neural networks", *Earthq. Eng. Struct. D.*, **27**, 377-396.

Ghodrati Amiri, G., Ashtari, P. and Rahami, H. (2006), "New development of artificial record generation by wavelet theory", *Struct. Eng. Mech.*, **22**(2), 185-195.

Iyama, J. and Kuwamura, H. (1999), "Application of wavelets to analysis and simulation of earthquake

motions", *Earthq. Eng. Struct. D.*, **28**, 255-272.
Lee, S.C. and Han, S.W. (2002), "Neural-network-based models for generating artificial earthquakes and response spectra", *Comput. Struct.*, **80**, 1627-1638.
Lin, C.J. and Ghaboussi, J. (2000), "Recent progress on neural network based methodology for generating artificial earthquake accelerograms", *Proc. of the 12th World Conf. on Earthquake Engineering,* Auckland, New Zealand, 29 Jan.-5 Feb.
MacCann, W.M. and Shah, H.C. (1979), "Determining strong-motion duration of earthquake", *B. Seismol. Soc. Am.*, **69**, 1253-1265.
MATLAB Reference Guide (1999), The Math Works Inc.
Mukherjee, S. and Gupta, K. (2002), "Wavelet-based characterization of design ground motions", *Earthq. Eng. Struct. D.*, **31**, 1173-1190.
Naeim, F. (1999), *The Seismic Design Handbook*, Van Nostrand.
Newland, D.E. (1994), Random Vibrations, Spectral and Wavelet Analysis, 3rd Edition, Longman Singapore Publishers.
Park, J. and Sandberg, J.W. (1991), "Universal approximation using radial basis functions network"", *Neural Comput.* **3**, 246-257.
Rajasekaran, S., Latha, V. and Lee, S.C. (2006), "Generation of artificial earthquake motion records using wavelets and principal component analysis", *J. Earthq. Eng.,* **10**(5), 665-691.
Ramezi, H. (1997), Base Accelerogram Data of Iranian Accelerograph Network, Building and Housing Research Center, BHRC-PN S 253, Tehran, Iran.
Zhou, Z. and Adeli, H. (2003), "Wavelet energy spectrum for time-frequency localization of earthquake energy", *Comput. Aided Civil Infrastruct. Eng.*, **13**, 133-140.

Notation

A_j : Approximation at level j
$a_g(t)$: Ground acceleration
CWT : Continuous wavelet transform
cA : Scaling coefficients
cD : Wavelet coefficients
c_j : jth coefficient of basis function
DWT : Discrete wavelet transform
D_j : Detail at level j
FFT : Fast Fourier transform
f : Center frequency
f(t) : Signal
k : Parameter
N : Order
N : Parameter
PSA : Pseudo-acceleration response spectrum
PSV : Pseudo-velocity response spectrum
RBF : Radial basis function
T : Period
t : Time
WMRA : Wavelet multiresolution analysis
x : Displacement
$\dot{x}$: Velocity
$\ddot{x}$: Acceleration
Z : Set of positive integers
Δt : Time interval
$\phi(t)$: Scaling function

ξ : Damping coefficient of the SDOF
ψ : Basis function
ω : Fundamental frequency of the SDOF